© 2018 Hefei Institutes of Physical Science, Chinese Academy of Sciences and IOP Publishing Printed in China and the UK

Plasma Sci. Technol. **20** (2018) 065512 (11pp) https://doi.org/10.1088/2058-6272/aab301

Applying chemical engineering concepts to non-thermal plasma reactors

Pedro AFFONSO NOBREGA[1], Alain GAUNAND[2], Vandad ROHANI[1], François CAUNEAU[1] and Laurent FULCHERI[1]

[1] MINES ParisTech, PSL Research University, PERSEE—Centre for Processes, Renewable Energy and Energy Systems, CS 10207 rue Claude Daunesse F-06904 Sophia Antipolis Cedex, France
[2] MINES ParisTech, PSL Research University, CTP—Centre for Thermodynamics of pProcesses, 35 rue St Honoré F-77300 Fontainebleau, France

E-mail: pedro.affonso_nobrega@mines-paristech.fr

Received 25 January 2018, revised 9 February 2018
Accepted for publication 28 February 2018
Published 2 May 2018

Abstract

Process scale-up remains a considerable challenge for environmental applications of non-thermal plasmas. Undersanding the impact of reactor hydrodynamics in the performance of the process is a key step to overcome this challenge. In this work, we apply chemical engineering concepts to analyse the impact that different non-thermal plasma reactor configurations and regimes, such as laminar or plug flow, may have on the reactor performance. We do this in the particular context of the removal of pollutants by non-thermal plasmas, for which a simplified model is available. We generalise this model to different reactor configurations and, under certain hypotheses, we show that a reactor in the laminar regime may have a behaviour significantly different from one in the plug flow regime, often assumed in the non-thermal plasma literature. On the other hand, we show that a packed-bed reactor behaves very similarly to one in the plug flow regime. Beyond those results, the reader will find in this work a quick introduction to chemical reaction engineering concepts.

Keywords: non-thermal plasma, chemical engineering, dielectric barrier discharge (DBD), corona discharge, plug flow reactor, volatile organic compounds

1. Introduction

According to the 2017 Plasma Roadmap [1], 'process selectivity, conversion and/or energy efficiency are still not sufficient to justify the large-scale use of non-thermal plasmas' for many environmental applications. Examples of such applications include the conversion of CO_2 [2–5], the production of syngas or hydrogen [6–9], liquid fuels [10–12], ozone [13–15] or the removal of volatile organic compounds or other pollutants from air streams [16–21]. These applications usually involve the use of a plasma reactor where both desired and undesired reactions may take place during or following a non-equilibrium electric discharge, eventually with the help of a catalyst. Most studies in non-thermal plasma literature try to optimise selectivity, conversion and/or energy efficiency by acting on:

- the inlet parameters, such as gas temperature, composition or flow rate;
- the plasma parameters, such as the applied voltage waveform, its amplitude and frequency, the electrode configuration or the type of discharge (gliding-arc, dielectric barrier discharge, corona);
- the catalyst, its support and its position with respect to the discharge.

On the other hand, very few studies evaluate the impact of the reactor's geometry and its hydrodynamic characteristics on the process efficiency. Two main reasons may explain that. First, changing the geometrical parameters of a laboratory reactor requires the fabrication of a new reactor or a more complicated modular design. Second, non-equilibrium plasma processes usually involve a wide range of spatial and temporal scales, as well as complex kinetic mechanisms. This makes the coupling with computational fluid dynamic models and therefore the numerical investigation of the hydrodynamics of a plasma reactor rather challenging (nevertheless, we can find such studies in [13, 22]). But filling the

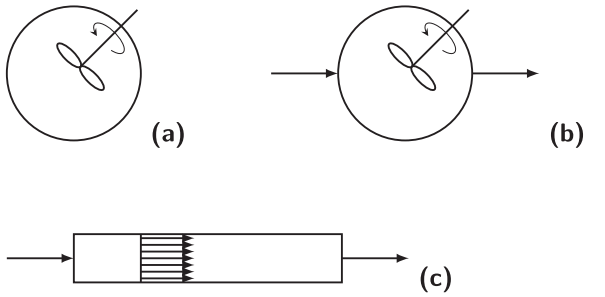

Figure 1. Some different reactor models used in chemical engineering mentioned in this paper: batch reactor (a), continuously stirred tank reactor (b), plug flow reactor (c).

gap in our knowledge of how the hydrodynamics and the geometry of the reactor may impact the performance of a plasma process is a fundamental step not only towards process scale-up, but also towards a better understanding of laboratory experimental results.

Chemical reaction engineering, a branch of chemical engineering concerned with the design and operation of classical chemical reactors, could help us in filling this gap. Indeed, chemical reaction engineering is a well-established discipline, with lots of concepts and methods developed for the design, the modelling and the understanding of homogeneous or heterogeneous reactors. Most interestingly, some simple analytical results in chemical reaction engineering provide powerful insights for the design of chemical reactors. In this work, we try to extend these results to plasma reactors.

Our study is not the first one to look into how hydrodynamic aspects can impact the chemical performance of plasma reactors or to apply chemical engineering concepts to such reactors. For instance, Gonzalez-Aguilar *et al* [8] model the reforming of n-octane in a non-thermal plasma torch by a network of 0D well-stirred reactors (WSRs) and plug flow reactors (PFRs) to represent the hydrodynamics of the torch. Similarly, Lietz and Kushner [23] use two 0D WSRs to model the plasma treatment of liquid-covered tissue. More generally, Pinhão *et al* [6] describe the influence that gas expansion inside a non-thermal plasma PFR may have on process parameters such as the residence time, the specific energy input (SEI) or the material balances. Also, Meichsner *et al* [24] present some non-thermal plasma reactor models: the plug flow model, the back-mixing model and the closed reactor model, which we call in this paper PFR, continuously stirred tank reactor (CSTR) and batch reactor, respectively. Bogaerts *et al* [25] explicitly mentions the equivalence between the batch and the PFR as a convenience for the modelling of plasma reactors.

Researchers in the plasma domain often use a batch reactor model when studying detailed kinetic mechanisms [15, 26, 27] or a PFR model when interested in global quantities such as removal or yield rates [28–30]. Further, sometimes the PFR model is implicitly assumed, without any mention of it [31–34]. However, the PFR hypothesis does not necessarily hold, as most of the plasma reactors at laboratory scale have a low Reynolds number, being closer to the laminar regime than to the plug flow regime, which requires turbulence to homogenise the fluid in the cross-flow direction and/or a very long tube (high aspect ratio), as we will see in the following. Further, electro-hydrodynamic effects such as the so-called 'ionic wind' may induce flow recirculation [35–37].

In this context, we attempt to propose a short and accessible introduction to chemical reaction engineering to the plasma community. The goal is to make easily available some basic concepts which are essential to the design of plasma reactors, but also to the analysis of experimental results. Moreover, we seek to show with simple analytical models how reactor hydrodynamics may have an important impact on non-thermal plasma reactors for environmental applications. In particular, we use the treatment of atmospheric pollutants by non-thermal plasmas as an example, adopting a simplified kinetic model to evidence that impact.

2. Basic chemical reaction engineering concepts

Chemical reaction engineering deals with transformation and transfer processes taking place inside a reactor. Such processes may be impacted by the nature of reactants and inlet conditions, as well as reaction thermodynamics and kinetics, hydrodynamics, circulation and mixing inside the reactor or heat transfer within and across the reactor's walls [38]. Outlet products and conditions will then be intimately related to all those aspects.

2.1. Ideal reactors

With the goal of simplifying the approach to complex real reactors, ideal reactor configurations may be analysed. Three of the simplest configurations are the batch reactor or WSR, the CSTR and the PFR. They are shown in figure 1.

In a batch reactor, a certain quantity of mass reacts over time with perfect mixing of the reactor's content. Due to the perfect mixing, all properties in the reactor such as species concentrations and temperature are uniform. Without inlet or outlet fluxes, the species balance can be written [38, 39]:

$$\frac{\mathrm{d}n_j}{\mathrm{d}t} = V\dot{\omega}_j \tag{1}$$

$$n_j(t=0) = n_{j0} \tag{2}$$

where n_j is the number of moles of species j inside the reactor, V the volume of the latter and $\dot{\omega}_j$ the rate of production of moles of j per volume. $\dot{\omega}_j$ is given by:

$$\dot{\omega}_j = \sum_i \nu_{ij} r_i \tag{3}$$

where ν_{ij} is the number of moles of j produced (or destroyed if negative) per mole of reaction i, whose rate is r_i.

The CSTR is similar to a batch reactor, but working in a continuous manner, with inlet and outlet flows. It can be considered to be in a stationary regime, which is often a good approximation of real conditions. Similarly to the batch

reactor, properties are uniform in the CSTR due to the perfect mixing. Logically, outlet properties are the same as those inside the reactor. The species balance is then written [38, 39]:

$$F_{j,\text{in}} + V\dot{\omega}_j = F_{j,\text{out}} \tag{4}$$

where $F_{j,\text{in/out}}$ are the inlet and outlet molar flow rates of j.

In the PFR, the reacting fluid flows in a tube without axial dispersion. All properties inside the reactor, including the flow velocity or species concentrations, are supposed to be uniform in a given cross-section of infinitesimal thickness dx. In this case, the species balance is written [38, 39]:

$$\frac{\mathrm{d}F_j}{\mathrm{d}x} = S\dot{\omega}_j \tag{5}$$

where S is the cross-sectional area of the tube. Further, the following boundary conditions apply:

$$F_j(x = 0) = F_{j,\text{in}} \tag{6}$$

$$F_{j,\text{out}} = F_j(x = L) \tag{7}$$

where L is the length of the tube. We can learn more in the case of a single first-order reaction of type $A \rightarrow B$ with rate $r = kC_A$, where C_A is the concentration of A. For the sake of simplicity, we consider the rate constant k to be fixed. In that case, the concentration C_A can be obtained for each type of reactor according to equations (1), (4) and (5), respectively [38, 39]:

$$\text{Batch:} \quad C_A/C_{A0} = \exp(-kt) \tag{8}$$

$$\text{CSTR:} \quad C_A/C_{A,\text{in}} = 1/(1 + k\tau) \tag{9}$$

$$\text{PFR:} \quad C_A/C_{A,\text{in}} = \exp(-k\tau) \tag{10}$$

where $\tau = V/Q$ is the so-called space time (Q is the inlet flow rate).

From equations (8) and (9) we can see that a batch flow reactor and a PFR are analogous, as if there is no change of fluid density with pressure, temperature or composition (due to reactions), t and τ are equivalent. It means that experimental results obtained with a batch reactor can be transposed to a PFR with the same residence time. Further, from equations (9) and (10) we can show that for a first order reaction, conversion of A is higher with a PFR than with a CSTR for the same value of τ [38, 39]. In general, for a reaction $A \rightarrow$ products with reaction order n (and without changes in fluid density), higher conversion of A is obtained with a PFR if $n > 0$ and with a CSTR if $n < 0$ if τ is fixed. Conversions with PFR and CSTR are equal in case $n = 0$.

Finally, it is important to note that $k\tau$ is the main parameter governing conversion in both CSTR and PFR. This parameter is the so-called Damköhler number Da, which gives the ratio between the flow and the chemistry characteristic times. In general, for a nth order reaction, the Damköhler number is defined as $Da = k_n C_{A,\text{in}}^{n-1}\tau$.

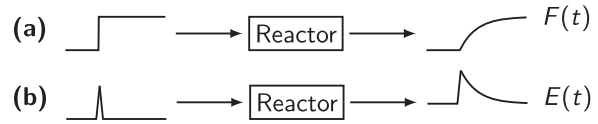

Figure 2. Scheme of tracer step (a) and impulse (b) responses of a reactor and their relation to $E(t)$ and $F(t)$.

Table 1. Dimensionless residence time distributions (RTDs) $E_\theta(\theta)$ obtained analytically [39, 40].

Reactor type	$E_\theta(\theta)$
CSTR	$\exp(-\theta)$
PFR	$\delta(\theta - 1)$
N CSTR in series	$N\frac{(N\theta)^{N-1}}{(N-1)!}\exp(-N\theta)$
LFR—circular tube	$\begin{cases} 0, & \theta < 1/2 \\ \frac{1}{2\theta^3}, & \theta \geqslant 1/2 \end{cases}$
LFR—parallel plates	$\begin{cases} 0, & \theta < 2/3 \\ \frac{1}{3\theta^3}\left(1 - \frac{2}{3\theta}\right)^{-0.5}, & \theta \geqslant 2/3 \end{cases}$

2.2. Non-ideal reactors

2.2.1. Residence time distribution. Real reactors always differ from ideal PFRs or CSTRs because of existing recirculation and channelling of fluid and stagnation zones, no matter what efforts are made to approach either of these ideal configurations. One of the means to account for these non-ideal behaviours are residence time distributions (RTDs).

The RTD $E(t)$ corresponds to the fraction of fluid which stays in the reactor for a time between t and $t + \mathrm{d}t$. If a tracer is introduced at the inlet of the reactor and its concentration measured at the outlet, the RTD corresponds to the response to an impulse input. That could be a droplet of colourant introduced in the inlet, for instance. The response to a step input is denoted by $F(t)$ and is related to $E(t)$ by:

$$F(t) = \int_0^t E(t')\,\mathrm{d}t'. \tag{11}$$

Figure 2 is a scheme of both impulse and step response experiments. RTDs obtained experimentally are useful to diagnose the existence of recirculation, channelling of fluid and stagnation zones, as well as to develop a flow model for the reactor. More information on that can be found on [39, 40].

Some common RTDs obtained analytically for a variety of reactors are given in the equations in table 1. They are given in dimensionless form $E_\theta(\theta) = \tau E(t)$, where $\theta = t/\tau$. The corresponding dimensionless step responses $F(\theta) = F(t)$ are given in table 2 and shown in figure 3 as an illustration. LFR refers to laminar flow reactors, which will be described in section 3.4.1.

Under certain hypotheses, it can be shown that the conversion for any reactor can be found from the conversion

Table 2. Dimensionless step responses $F(\theta)$ obtained analytically [39, 40].

Reactor type	$F(\theta)$
CSTR	$1 - \exp(-\theta)$
PFR	$\begin{cases} 0, & \theta < 1 \\ 1, & \theta > 1 \end{cases}$
N CSTR in series	$1 - \exp(-N\theta)\left[1 + N\theta + \frac{(N\theta)^2}{2!} + \cdots + \frac{(N\theta)^{N-1}}{(N-1)!}\right]$
LFR—circular tube	$\begin{cases} 0, & \theta < 1/2 \\ 1 - \frac{1}{4\theta^2}, & \theta \geqslant 1/2 \end{cases}$
LFR—parallel plates	$\begin{cases} 0, & \theta < 2/3 \\ \left(1 + \frac{1}{3\theta}\right)\left(1 - \frac{2}{3\theta}\right)^{0.5}, & \theta \geqslant 2/3 \end{cases}$

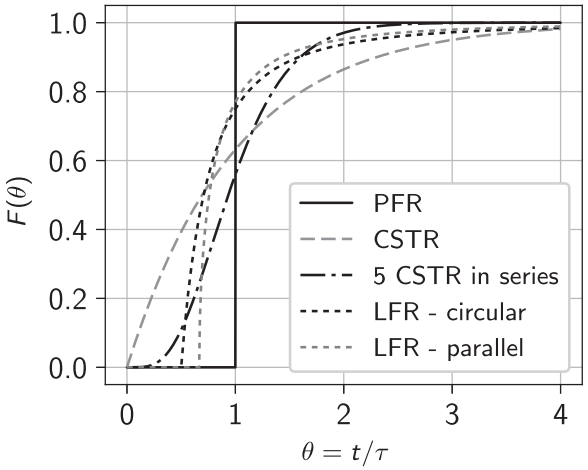

Figure 3. Tracer step responses for $F(\theta)$ for different reactor models. $F(\theta)$ expressions are given in table 2.

in a batch reactor and the RTD:

$$\frac{C_A}{C_{A,\text{in}}} = \int_0^{+\infty} \left(\frac{C_A}{C_{A,\text{in}}}\right)_{\text{batch}} E(t)\,\mathrm{d}t = \int_0^{+\infty} \left(\frac{C_A}{C_{A,\text{in}}}\right)_{\text{batch}} E_\theta(\theta)\,\mathrm{d}\theta. \tag{12}$$

Equation (12) is only valid for the so-called macrofluid regime, where small elements of fluid go through the reactor without mixing with each other. In this case, each of these elements behave as a tiny batch reactor. On the other hand, in the microfluid regime, small elements of fluid are very well mixed. The mathematical treatment of the microfluid regime is more complex than that for the macrofluid regime. For that reason, we will avoid it in the scope of this work, even though gases generally behave as microfluids. According to Villermaux [38], equation (12) may be used as a first approximation for the microfluid regime if $C_A/C_{A,\text{in}}$ is not very low. For instance, for a first order reaction, applying equation (8) to equation (12) would yield:

$$\frac{C_A}{C_{A,\text{in}}} = \int_0^{+\infty} \exp(-kt)E(t)\,\mathrm{d}t = \int_0^{+\infty} \exp(-kt)E_\theta(\theta)\,\mathrm{d}\theta. \tag{13}$$

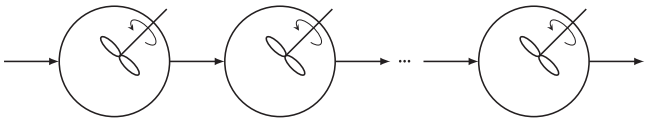

Figure 4. Scheme of CSTRs in series used to model axial dispersion.

The remarks made on section 2.1 are of major importance here: we can obtain the batch reactor conversion from a PFR.

2.2.2. Axial dispersion. Deviations from the ideal PFR model may occur in real reactors due to some mixing in the axial direction. This mixing may be due to a radial velocity profile, molecular diffusion in laminar flow, turbulent diffusion in turbulent flow or the irregular path of the fluid in a packed-bed reactor. This behaviour may be modelled by a diffusion coefficient D and the resulting species balance for species j is:

$$D\frac{\mathrm{d}^2 C_j}{\mathrm{d}x^2} - u\frac{\mathrm{d}C_j}{\mathrm{d}x} + \dot{\omega}_j = 0 \tag{14}$$

where u is the flow speed, supposed constant along the axial direction x. This is the so-called axial dispersion model, which can be used to model turbulent flow in pipes, laminar flow in long pipes or packed bed reactors. The importance of axial dispersion in the reactor behaviour is characterised by the dispersion number D/uL. If $D/uL \gg 1$, then dispersion dominates and the flow tends to be mixed. On the other hand, if $D/uL \ll 1$, convection dominates and the flow tends to behave as ideal plug flow. The reciprocal of the dispersion number is often called the Péclet number, even though this nomenclature should be applied only when the diffusion coefficient accounts for molecular diffusion alone. Correlations for the value of D can be found in Perry's Chemical Engineers' Handbook [41] and in [40]. Solving equation (14) may be quite complicated depending on the boundary conditions and the reaction rate dependency on C_j. An alternative model is to use a number N of CSTRs of volume V_i in series where the total space time is equal to the sum of the space time of each reactor:

$$\tau = \frac{V}{Q} = N\tau_i = \frac{NV_i}{Q}. \tag{15}$$

Figure 4 shows a scheme of the tank-in-series model, as it is also called: Villermaux [38] suggests the following relation between N and the dispersion number D/uL:

$$N = \frac{1}{2}\left(\frac{uL}{D}\right) + 1. \tag{16}$$

According to that author, if we put aside the physical meaning of the tank-in-series model, a non-integer value of N can be used by replacing the factorial term in the RTD given in table 2 by the Gamma function:

$$(N-1)! = \Gamma(N) = \int_0^{+\infty} x^{N-1}\exp(-x)\,\mathrm{d}x. \tag{17}$$

With this approach, Villermaux [38] states that equivalence between equation (14) and the tank-in-series model is 'excellent' for $N > 50$. In any case, several authors

recommend the use of the tank-in-series model rather than the axial dispersion model due to its greater simplicity.

3. Application to pollutant removal by non-thermal plasmas

If the hydrodynamics of the reactor can significantly impact the performance of a reactor for a simple homogeneous reaction, that should also be the case for any plasma reactor. In this section, we will use the concepts presented above to analyse non-thermal plasma reactors. We focus on the use of such reactors for the removal of small concentrations of pollutants from air streams, one of the promising environmental applications of non-thermal plasmas.

3.1. A simplified model for PFRs and definition of a Damköhler number

In our analysis, we make use of the four-reaction simplified kinetic model proposed by Rosocha and Korzekwa [31] and Yan *et al* [42]:

$$\text{Radical production} \qquad M \rightarrow R \qquad r = G\bar{P} \tag{18}$$

$$\text{Pollutant removal} \qquad X + R \rightarrow A \qquad r = k_X C_X C_R \tag{19}$$

$$\text{Radical linear termination} \qquad M + R \rightarrow B \qquad r = k_M C_M C_R \tag{20}$$

$$\text{Radical non}-\text{linear termination} \qquad R + R \rightarrow C \qquad r = k_{RR} C_R^2 \tag{21}$$

where $\bar{P} = P/V$ is the specific power input, with P the power dissipated in the plasma and V the reactor volume, k_X, k_M and k_{RR} are the reaction rate constants for equations (19) to (21), C_X, C_R and C_M the concentrations of X, R and M, respectively, and G the number of radicals produced per energy unit. For the sake of simplicity, we assume the following hypotheses:

- Reaction rate constants, the gas density or the specific power input are constant and do not vary, particularly with temperature. In reality, if some amount of the dissipated plasma power is converted to heat, and heat transfer from the reactor to the environment is not efficient, temperature variations can be significant inside the reactor. In such a situation, this hypothesis may not hold.
- The gas density does not change due to reactions. Gas density changes due to reactions are indeed negligible if we consider that at most a few parts per thousand of radicals are produced and of pollutants are removed.
- The concentration C_M does not change due to reactions.
- Radicals are continuously produced in the whole reactor volume.
- Radical concentration is low and therefore, radical non-linear termination is not a significant pathway for radical loss. In other words, $k_M C_M C_R \gg k_{RR} C_R^2$.
- Radical concentration is stationary. That means that radicals produced by the plasma are consumed instantaneously either by pollutant removal or radical linear termination reactions. We can then write:

$$\frac{\mathrm{d}C_R}{\mathrm{d}t} = G\bar{P} - k_X C_X C_R - k_M C_M C_R = 0 \tag{22}$$

$$C_R = \frac{G\bar{P}}{k_X C_X + k_M C_M}. \tag{23}$$

From equation (19) we can obtain the pollutant removal rate:

$$\dot{\omega}_X = \frac{\mathrm{d}C_X}{\mathrm{d}t} = -k_X C_X C_R = -\frac{k_X C_X G\bar{P}}{k_X C_X + k_M C_M}. \tag{24}$$

We use normalised variables:

$$\xi = C_X / C_{X,\mathrm{in}} \tag{25}$$

$$z = k_M C_M / k_X C_{X,\mathrm{in}} \tag{26}$$

where $C_{X,\mathrm{in}}$ is the pollutant's inlet concentration. $\xi = C_X/C_{X,\mathrm{in}}$ is commonly called the residual fraction of X. The *SEI*, which is a widely used parameter in plasma applications, can be obtained from the specific power input by:

$$\mathrm{d}SEI = \bar{P}\,\mathrm{d}t \tag{27}$$

$$SEI = \bar{P}\tau. \tag{28}$$

We rewrite equation (24) by applying equations (25) to (27):

$$\frac{\mathrm{d}\xi}{\mathrm{d}SEI} = -\frac{\xi}{\xi + z}\frac{G}{C_{X,\mathrm{in}}}. \tag{29}$$

We can then define the characteristic energy as:

$$\beta = C_{X,\mathrm{in}}(1 + z)/G \tag{30}$$

and a Damköhler number:

$$Da = \frac{SEI}{\beta} = \frac{G\bar{P}\tau}{C_{X,\mathrm{in}}(1 + z)} \tag{31}$$

to obtain the final normalised form of the pollutant removal rate:

$$\frac{\mathrm{d}\xi}{\mathrm{d}Da} = -\frac{\xi(1 + z)}{\xi + z}. \tag{32}$$

We may analyse the importance of each parameter. The value of z defined by equation (26) gives the relative importance of radical loss by linear termination and by the pollutant removal reaction. If $z \gg 1$ radical linear termination dominates. On the contrary, if $z \ll 1$ pollutant removal is the main mechanism for radical loss. From equation (32) we can see that the pollutant removal has respectively either a first order or a zero order behaviour in these limits. Table 3 summarises this analysis.

Table 3. Summary of dominant mechanisms for radical loss depending on the ratio z.

Value of z	Dominant mechanism for radical loss	Pollutant removal rate	Reaction order
$z \gg 1$	Radical linear termination	$\frac{\mathrm{d}\xi}{\mathrm{d}Da} = -\xi$	First order
$z \ll 1$	Pollutant removal	$\frac{\mathrm{d}\xi}{\mathrm{d}Da} = -1$	Zero order

Another important parameter is the characteristic energy β. This parameter is very often used in plasma literature [19, 31, 32, 42–44] as an indicator of the efficiency of pollutant removal by a non-thermal plasma process. It corresponds to the energy needed to decompose 63.2% of the pollutant's initial concentration. It can be obtained from plots of log ξ as a function of the SEI. Indeed, experimental results show that the residual fraction ξ usually follows an exponential decay $\exp(-SEI/\beta)$, at least for values of ξ close to unity (>80%). One of the advantages of the mechanism model described by equations (18) to (21) is that it allows us to reproduce that behaviour, as we will see in the next session.

Finally, Da gives the ratio between the SEI and the characteristic energy β. The numerator is the product of the specific power input $\bar{P}$ and the space time τ. The denominator can be viewed as the product of the same specific power input $\bar{P}$ by a chemistry characteristic time τ_c. The plasma Damköhler number Da is therefore a ratio between flow and chemistry characteristic times:

$$Da = \frac{\mathrm{SEI}}{\beta} = \frac{\bar{P}\tau}{\bar{P}\tau_c} = \frac{\tau}{\tau_c}. \tag{33}$$

The main advantage of using the Damköhler number is that it allows a quick comparison with chemical engineering concepts, where this dimensionless number is widely used.

3.2. Pollutant removal in a PFR

The first kind of reactor we analyse is the PFR. Beyond the fact that it is one of the simplest ideal reactor models used in chemical engineering, most non-thermal plasma reactors for pollutant removal have a tubular shape and are often compared to a PFR, implicitly or explicitly [28–34]. However, Trambouze [45] suggests that a PFR requires the following conditions on Reynolds number Re and aspect ratio L/d_t:

$$Re = ud_t/\nu > 10^4 \tag{34}$$

$$L/d_t > 100 \tag{35}$$

where d_t is the tube's inner diameter and ν the kinematic viscosity of the fluid. Rosocha and Korzekwa [31] implicitly used a PFR model to integrate equation (24) and obtain an expression for ξ. Indeed, combining equations (24) and (5), we have the balance for the pollutant X in a PFR:

$$\frac{\mathrm{d}F_X}{\mathrm{d}x} = S\dot{\omega}_X = -\frac{k_X C_X G\bar{P}S}{k_X C_X + k_M C_M}. \tag{36}$$

If there is no density change, the flow velocity inside the reactor is the same, so that we can write $\mathrm{d}F_X = uS\,\mathrm{d}C_X$ and $\mathrm{d}x = u\,\mathrm{d}t$. Equation (36) is therefore equivalent to equation (24), and as a consequence, to equation (32). We can rearrange the latter in order to integrate with initial conditions $\xi = 1$ and $Da = 0$:

$$\frac{1}{1+z}\int_1^{\xi}\left(\frac{\xi' + z}{\xi'}\right)\mathrm{d}\xi' = -\int_0^{Da}\mathrm{d}Da' \tag{37}$$

which yields after integration:

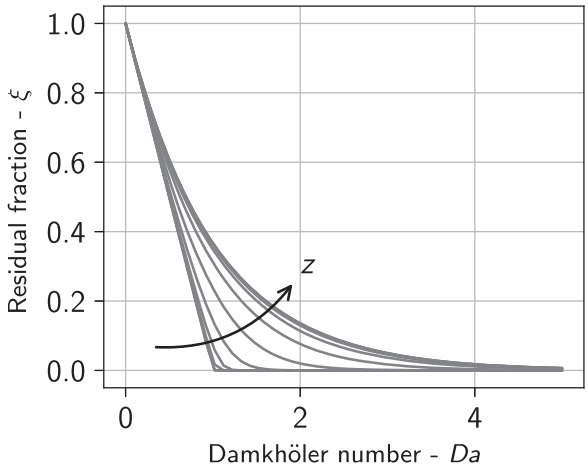

Figure 5. Residual fraction ξ of X as a function of the Damköhler number $Da = SEI/\beta$ for a PFR. Different curves represent different values of z, logarithmically ranging from 10^{-3} to 10^3 and increasing according to the direction of the arrow.

$$\frac{\xi - 1}{z+1} + \frac{z}{z+1}\ln\xi = -Da. \tag{38}$$

This is the same expression obtained by Rosocha and Korzekwa [31]. One needs to solve it in order to find the residual fraction ξ at the outlet of the reactor for a given Damköhler number Da and a given value of z. Some remarks:

- If ξ is close to unity, which means low pollutant removal:

$$\ln\xi = (\xi - 1) - \frac{(\xi-1)^2}{2} + \frac{(\xi-1)^3}{3} - \cdots \approx (\xi - 1) \tag{39}$$

  and in that case equation (38) reduces to

$$\ln\xi = -Da \tag{40}$$

  or in a widely known form:

$$\xi = \frac{C_X}{C_{X,\mathrm{in}}} = \exp\left(-\frac{SEI}{\beta}\right). \tag{41}$$

  This is the exponential decay law observed experimentally for low conversion.
- If $z \gg 1$ or $z \ll 1$, we have respectively the PFR first order and zero order behaviours:

$$\xi = \exp(-Da) \tag{42}$$

$$\xi = 1 - Da. \tag{43}$$

Figure 5 shows the residual fraction ξ as a function of the Damköhler number $Da = SEI/\beta$ for different values of z for a PFR (obtained from equation (38)). z values are logarithmically spaced from 10^{-3} to 10^3. The arrow indicates the direction of increase of z. For $z \ll 1$, the curves come close to the zero order behaviour defined by the linear function given by equation (43). Conversely, when $z \gg 1$, the curves

approximate the first order behaviour given by equation (42) for a PFR.

3.3. Pollutant removal in a non-ideal reactors

From the pollutant removal in a PFR, we can obtain the pollutant removal in non-ideal reactors if the RTD is known. Applying changes of variables $\theta = t/\tau$ and $\xi = C_X/C_{X,\text{in}}$ to equation (12) we obtain:

$$\xi = \int_0^{+\infty} \xi_{\text{batch}}(\theta) E_\theta(\theta)\, \mathrm{d}\theta \tag{44}$$

where $\xi_{\text{batch}}(\theta)$ is the residual fraction obtained with a batch reactor after a reduced time θ. As we have seen in section 2.1, if there is no change of density in the fluid, that residual fraction is the same as the one obtained with a PFR with a residence time which corresponds to a Damköhler number $Da_t = \theta Da$, as made explicit below:

$$Da_t = \frac{G\overline{P}t}{C_{X,\text{in}}(1+z)} = \frac{t}{\tau}\frac{G\overline{P}\tau}{C_{X,\text{in}}(1+z)} = \theta Da. \tag{45}$$

We can then write equation (12) for pollutant removal:

$$\xi = \int_0^{+\infty} \xi_{\text{PFR}}(\theta Da) E_\theta(\theta)\, \mathrm{d}\theta \tag{46}$$

where ξ_{PFR} may be obtained from equation (38):

$$\frac{\xi_{\text{PFR}} - 1}{z+1} + \frac{z}{z+1}\ln\xi_{\text{PFR}} = -\theta Da. \tag{47}$$

3.4. Some reactor configurations used in environmental applications of non-thermal plasmas

The reader familiar with the literature of non-thermal plasma for environmental applications will notice that conditions for a plug flow behaviour given by equations (34) and (35) are not always satisfied in laboratory-scale reactors. For instance, the reactor used by Takaki *et al* [46] operates with a Reynolds number of 25.7, being clearly in a laminar regime. In this section, we analyse two common types of reactors used in studies of pollutant removal by non-thermal plasmas: the laminar flow reactor and the packed-bed reactor.

3.4.1. Laminar flow reactor. Laminar flow in a tube is a common configuration for non-thermal plasma reactors in laboratory, where flow rates are small ($Re < 2300$). Laminar flow is characterised by a parabolic velocity profile as schematised in figure 6.

Three different models may be used to represent a laminar flow depending on flow conditions according to Levenspiel [40]. These flow conditions are characterised by the Bodenstein number and the aspect ratio. The Bodenstein number is given by

Figure 6. Scheme of a laminar flow reactor with a parabolic velocity profile.

Table 4. Numerical values used in the analysis of the circular tube reactor.

Parameter	Symbol	Value
Molecular diffusion coefficient	D_m	$0.2\ \text{cm}^2\ \text{s}^{-1}$
Inlet flow rate	Q	1 l/min
Inlet speed	u	$0.11\ \text{m}\ \text{s}^{-1}$
Hydraulic diameter	d_t	14 mm
Tube's length	L	140 mm
Bodenstein number	$Bo = ud_\text{t}/D_\text{m}$	76
Aspect ratio	L/d_t	10

the product of the Reynolds number and the Schmidt number:

$$Bo = Re \cdot Sc = \frac{ud_\text{t}}{\nu} \cdot \frac{\nu}{D_\text{m}} \tag{48}$$

where D_m is the molecular diffusivity coefficient. The aspect ratio is given by the ratio between the tube's length L and its diameter d_t. Levenspiel suggests the following criteria for the choice of the laminar flow model [40]:

- For a short tube with high flow rate, the molecular diffusion effect is negligible and the flow is in a pure convection regime, with a parabolic velocity profile. This regime holds for $Bo > 450L/d_\text{t}$. In this case, one should use the RTDs given in table 1 for a laminar flow reactor, either circular tube or parallel plates.
- For a long tube, radial molecular diffusion tends to distort the parabolic profile and the axial dispersion model may be applied. This regime holds for $L/d_\text{t} > 6$ and $D/uL < 10$ and $Bo < 4L/d_\text{t}$. In that case, one should use the axial dispersion or tank-in-series model, with dispersion coefficient D given by equations (49) (circular tube) or (50) (parallel plates). If the tank-in-series model is used, N can then be obtained from equation (16).

$$\text{Circular tube:}\quad D = D_\text{m} + \frac{u^2 d_\text{t}^2}{192 D_\text{m}} \tag{49}$$

$$\text{Parallel plates:}\quad D = D_\text{m} + \frac{u^2 h^2}{210 D_\text{m}}. \tag{50}$$

- For very low flow rates, molecular diffusion dominates. We will not treat this case here as it seldom happens in plasma reactors. This regime holds for $D/uL < 10$.

In what follows, we analyse the impact of different models using a typical laboratory non-thermal plasma reactor as an example (taken from [33]). The reactor is considered to be an empty circular tube. This assumption neglects the effect of the central electrode on the flow, which should be taken

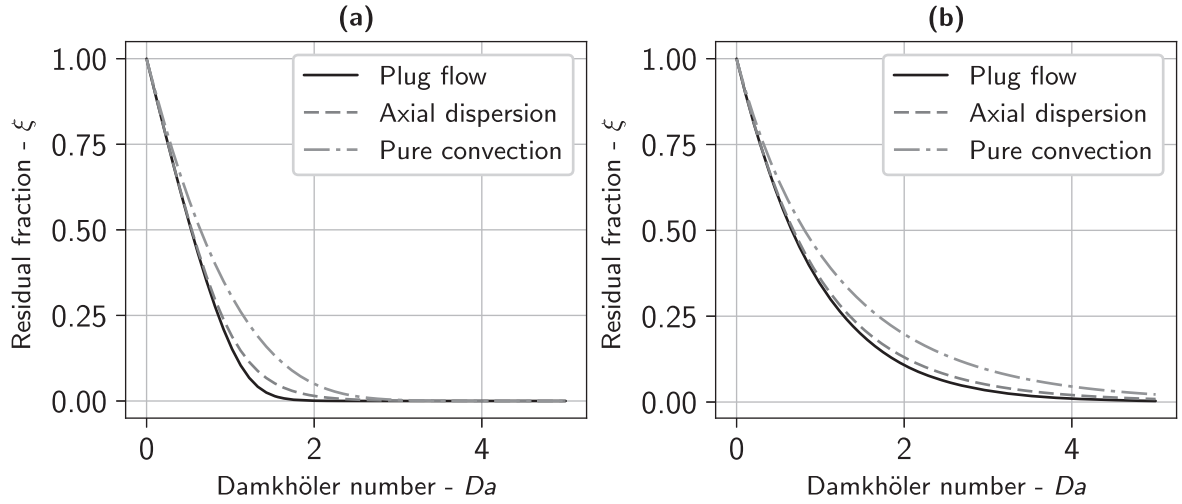

Figure 7. Residual fraction as a function of the Damköhler number for plug flow (PFR), axial dispersion/tank-in-series model and pure convection for $z = 0.2$ (a) and $z = 5.0$ (b).

Table 5. Numerical values for axial dispersion parameters.

Parameter	Symbol	Value
Dispersion coefficient	D	6.2 cm^2 s^{-1}
Dispersion number	D/uL	0.04
Number of CSTRs in series	N	13

into account in a more detailed analysis. The numerical values used are given in table 4.

We begin with the comparison between pure convection and axial dispersion regimes. Indeed, for the parameters given in table 4, the reactor should be in an intermediate regime between pure convection ($Bo > 450L/d_t = 4500$) and axial dispersion ($Bo < 4L/d_t = 40$), although closer to the latter. We obtain residual fractions by using equation (46). For pure convection, we apply the laminar flow reactor RTD given in table 1. For axial dispersion, we use a tank-in-series model, with RTD also given in table 1. The number of CSTRs in series is given by equation (16) for a dispersion coefficient D calculated from equation (49). The values for axial dispersion parameters D, D/uL and N are given in table 5.

Figure 7 shows the resulting comparison between pure convection and axial dispersion regimes for $z = 0.2$ (low z, close to zero order behaviour) and $z = 5.0$ (high z, close to first order behaviour). For both cases, we can see that in the axial dispersion regime (tank-in-series model) the residual fraction is closer to the one obtained with a PFR. That is due to the low value of the dispersion number D/uL. However, the difference between pure convection and PFR models is more significant, particularly for residual fractions under 0.50. The residual fraction for this reactor in an intermediate regime between axial dispersion and pure convection regimes is expected to be within the limits set by the corresponding curves in figure 7.

We now investigate the difference between two reactor shapes: circular tube and parallel plates. These two configurations have been used in laboratory experiments for removal of pollutants by non-thermal plasmas. Due to the different velocity profiles in circular and parallel plates (two-dimensional channel), the RTDs differ. Furthermore, correlations for axial dispersion coefficients are also different. Therefore, we should expect different performances for each reactor shape. For the parallel plates, we consider the same numerical values as those given in table 4 for a circular tube, but we replace the tube diameter d_t by the channel's height h and the corresponding hydraulic diameter $d_h = 2h$. The numerical values used as input are given in table 6. We consider $z = 5.0$.

Table 6. Numerical values used in the analysis of the parallel plates reactor.

Parameter	Symbol	Value
Channel's height	d_t	7 mm
Bodenstein number	$\mathrm{Bo} = ud_t/D_m$	76
Aspect ratio	L/d_t	10
Dispersion coefficient	D	1.6 cm^2 s^{-1}
Dispersion number	D/uL	0.01
Number of CSTRs in series	N	49

In figure 8, we see that there is little difference between residual fractions for circular tube and parallel plates in both axial dispersion and pure convection regimes, although the difference is more noticeable in the latter. Furthermore, for the axial dispersion regime, residual fractions for both circular tube and parallel plates are very close to the residual fraction for the PFR model.

3.4.2. Packed-bed reactor. Packed-bed reactors are much used in environmental applications of non-thermal plasmas, as coupling non-thermal plasma and heterogeneous catalysis may increase the performance of several processes [29, 47–49]. According to Villermaux [38], packed-bed reactors behave as PFRs if $L/d_p > 50$ and $L/d_t > 0.5$, where d_p is the diameter of the packing particles. But the packed-bed reactor may be subjected to some axial and radial dispersion due to the flow path in the void space left by the packing particles. According to Delgado [50], the axial dispersion coefficient is 5 times higher than the radial dispersion coefficient for a

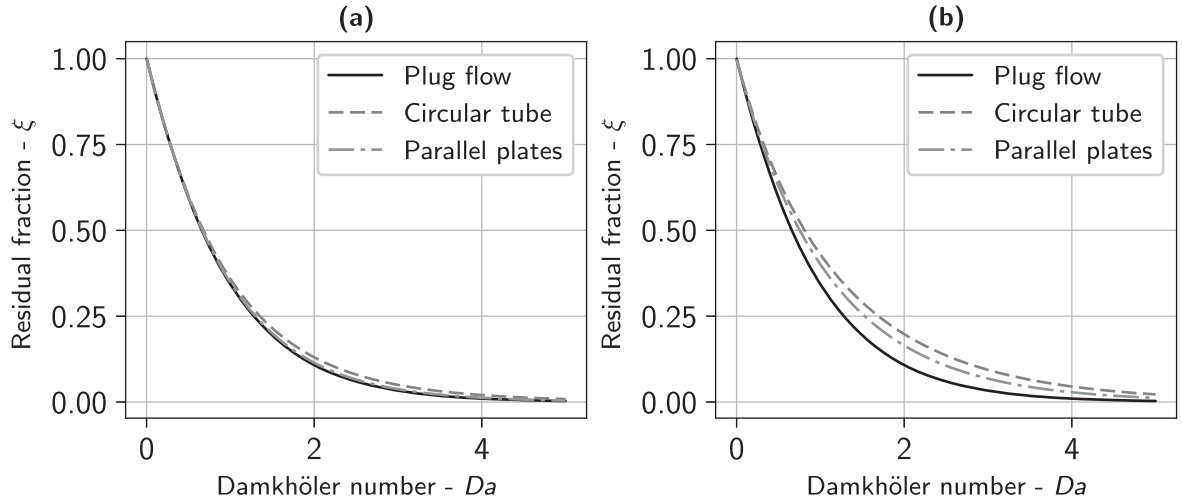

Figure 8. Residual fraction as a function of the Damköhler number for plug flow (PFR), circular tube and parallel plates for two different regimes: axial dispersion (a) and pure convection (b), for $z = 5.0$.

particle Reynolds number $Re = ud_p/\nu > 10$. Levenspiel [40] suggests using a tank-in-series model to account for axial dispersion in packed-bed reactors where the number of CSTRs in series is roughly $N \approx L/d_p$ if the fluid is a gas.

Chang and Lin [29] used a packed-bed reactor for removing toluene or acetone from an air stream. We take their reactor as an example. Its parameters are given in table 7. We also consider the hypothetical case where the reactor would have a length of 50 mm for comparison. Residual fractions are shown in figure 9 for $z = 0.2$ (a) and $z = 5.0$ (b). We can see that for both lengths, 50 mm and 140 mm, residual fractions for the packed-bed reactors are very close to the ones for an ideal PFR, even though the condition $L/d_p > 50$ proposed by Villermaux [38] is not satisfied.

If the choice $N \approx L/d_p$ can be used as a first approximation for modelling a packed-bed reactor, more detailed correlations to obtain the dispersion coefficient D (and hence N) are provided by Levenspiel [40] which take into account particle porosity or adsorption on the packing particles. Delgado [50] also provides correlations for the dispersion coefficient D that fit experimental data.

3.5. Model limitations

The application of chemical engineering concepts to non-thermal plasma reactors set out in this work presents several limitations in its current form. The first one is not taking into account the effects of temperature variations, especially the change of reaction rates and gas expansion inside the reactor. Temperature variations may indeed be significant due to the heat released by electric discharges. Another limitation is the assumption that radicals are continuously produced in the whole reactor volume. Most of the electric discharges used to produce non-thermal plasmas for environmental applications are rather filamentary and spatially heterogeneous. As a result, radicals are generated in a reduced fraction of the reactor volume. That leads to species concentration gradients, which may have an important impact on non-linear reaction rates. This is also true for heat, which may also be released in a reduced fraction of the reactor volume, leading to strong temperature gradients.

Table 7. Numerical values used in the analysis of the packed-bed reactor.

Parameter	Symbol	Value
Inlet flow rate	Q	0.6 l/min
Tube's diameter	d_t	20 mm
Tube's length	L	140 mm
Packing particle diameter	d_p	5 mm
Number of CSTRs in series	N	28

More detailed models could take into account the effects of temperature variations and spatial heterogeneity, but they would imply an increased complexity that we preferred to avoid in the scope of this work. To take into account temperature effects, one needs to know which fraction of the specific power $\bar{P}$ is converted to heat, how much heat is lost to the environment (heat transfer coefficient) and how reaction rates change with temperature (activation energies and/or temperature exponents). Plasma heterogeneity could be taken into account by using a reactor network model such as the one used by Gonzalez-Aguilar *et al* [8]. But in that case, one would need to define the volume of each reactor of the network and how they exchange mass and energy (diffusion coefficients). In all cases, modelling complexity quickly increases along with the number of input parameters, which are not necessarily available from experimental data and so must be guessed.

4. Conclusions

Hydrodynamics of non-thermal plasma reactors may have a significant impact on the performance of plasma processes. Fully understanding this impact helps us to design better plasma

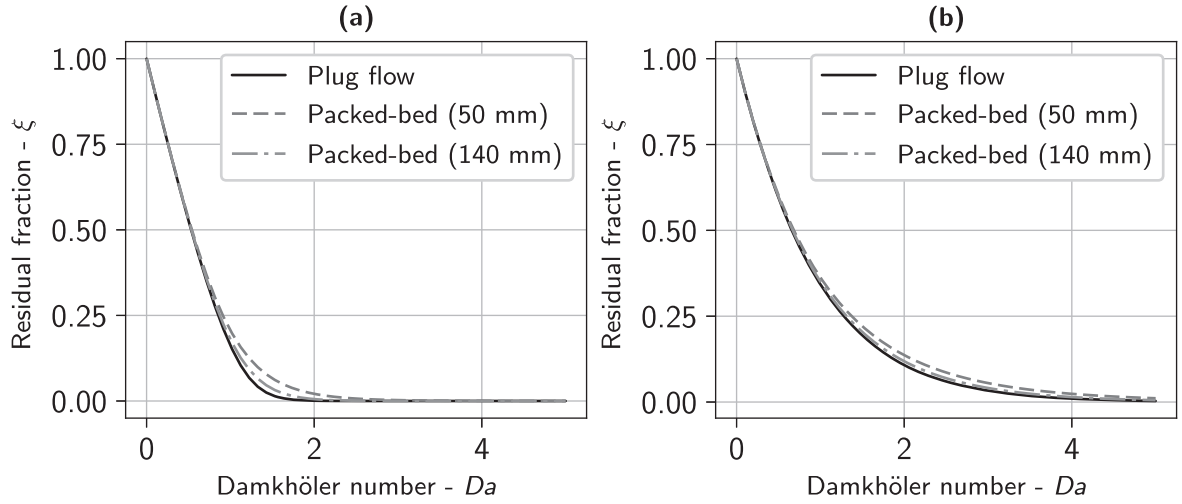

Figure 9. Residual fraction as a function of the Damköhler number for plug flow (PFR) and packed-bed reactors with lengths of 50 mm or 140 mm, for $z = 0.2$ (a) and $z = 5.0$ (b).

reactors, from laboratory to industrial scale, and to improve our comprehension of experimental results. Chemical engineering provides invaluable concepts to help understand how hydrodynamics affects chemical reactors in general. We applied some of these concepts to non-thermal plasma reactors in the particular context of pollutant removal by non-thermal plasmas. We did this by generalising the model originally proposed by Rosocha and Korzekwa [31] and Yan *et al* [42] for pollutant removal by non-thermal plasmas in PFRs to other reactor models. Furthermore, we defined a Damköhler number for the non-thermal plasma reactor, based on the SEI and the characteristic energy β. The Damköhler number allowed us to us establish a link with chemical engineering concepts, where this dimensionless number is widely used. We have shown that under certain conditions, a laminar flow reactor may behave differently from the plug flow model. This result deserves consideration since a number of laboratory scale non-thermal plasma reactors work in the laminar regime. On the other hand, we have shown that packed-bed reactors behave very similarly to PFRs. Even though the model used in our analysis is quite simple and does not take into account temperature variations or spatial heterogeneity, it is enough to give us an insight into how reactor hydrodynamics may impact its performance. Finally, we hope that this work will inspire more detailed analysis on plasma reactor hydrodynamics in a wider range of plasma applications.

Acknowledgments

Pedro Affonso Nobrega thanks the Provence-Alpes-Côte d'Azur (PACA) region for its contribution to his PhD scholarship.

ORCID iDs

Pedro AFFONSO NOBREGA https://orcid.org/0000-0001-5440-3700

References

[1] Adamovich I *et al* 2017 *J. Phys. D Appl. Phys.* **50** 323001
[2] Bak M S, Im S K and Cappelli M 2015 *IEEE Trans. Plasma Sci.* **43** 1002
[3] Ozkan A, Bogaerts A and Reniers F 2017 *J. Phys. D Appl. Phys.* **50** 084004
[4] Moss M S *et al* 2017 *Plasma Sources Sci. Technol.* **26** 035009
[5] Snoeckx R and Bogaerts A 2017 *Chem. Soc. Rev.* **46** 5805
[6] Pinhão N *et al* 2016 *Int. J. Hydrog. Energy* **41** 9245
[7] Nozaki T and Okazaki K 2013 *Catal. Today* **211** 29
[8] Gonzalez-Aguilar J *et al* 2009 *Energy Fuels* **23** 4931
[9] Rollier J D *et al* 2008 *Energy Fuels* **22** 1888
[10] Snoeckx R *et al* 2017 *Plasma Process. Polym.* **14** e1600115
[11] Eliasson B, Liu C J and Kogelschatz U 2000 *Ind. Eng. Chem. Res.* **39** 1221
[12] Al-Harrasi W S S, Zhang K and Akay G 2013 *Green Process. Synth.* **2** 479
[13] Chen J H and Davidson J H 2002 *Plasma Chem. Plasma Process.* **22** 495
[14] Malik M A *et al* 2015 *Plasma Chem. Plasma Process.* **35** 697
[15] Eliasson B, Hirth M and Kogelschatz U 1987 *J. Phys. D Appl. Phys.* **20** 1421
[16] Jarrige J and Vervisch P 2007 *Plasma Chem. Plasma Process.* **27** 241
[17] Koeta O *et al* 2012 *Plasma Chem. Plasma Process.* **32** 991
[18] Li Y Z *et al* 2014 *Plasma Chem. Plasma Process.* **34** 801
[19] Lovascio S *et al* 2015 *Plasma Chem. Plasma Process.* **35** 279
[20] Ogata A *et al* 2010 *Plasma Chem. Plasma Process.* **30** 33
[21] Vandenbroucke A M *et al* 2011 *J. Hazard. Mater.* **195** 30
[22] Castela M *et al* 2016 *Combust. Flame* **166** 133
[23] Lietz A M and Kushner M J 2016 *J. Phys. D Appl. Phys.* **49** 425204
[24] Meichsner J *et al* 2012 *Nonthermal Plasma Chemistry and Physics* (Boca Raton, FL: CRC Press)
[25] Bogaerts A *et al* 2017 *Plasma Process. Polym.* **14** e1600070
[26] Adamovich I V, Li T and Lempert W R 2015 *Philos. Trans. A Math. Phys. Eng. Sci.* **373** 20140336
[27] Kossyi I A *et al* 1992 *Plasma Sources Sci. Technol.* **1** 207
[28] Mok Y S and Nam I S 2002 *Chem. Eng. J.* **85** 87
[29] Chang C L and Lin T S 2005 *Plasma Chem. Plasma Process.* **25** 227
[30] Hsu D D and Graves D B 2003 *J. Phys. D Appl. Phys.* **36** 2898

[31] Rosocha L A and Korzekwa R A 1999 Removal of volatile organic compounds (VOCs) by atmospheric-pressure dielectric-barrier and pulsed-corona electrical discharges *Electrical Discharges for Environmental Purposes: Scientific Background and Applications* ed E M van Veldhuizen (Huntington, NY: NOVA Science Publishers)
[32] Jõgi I, Levoll E and Raud J 2016 *Chem. Eng. J.* **301** 149
[33] Blin-Simiand N, Pasquiers S and Magne L 2016 *J. Phys. D Appl. Phys.* **49** 195202
[34] Wang B W *et al* 2013 *J. Energy Chem.* **22** 876
[35] Feng J Q 1999 *J. Appl. Phys.* **86** 2412
[36] Moscosa-Santillan M *et al* 2008 *J. Clean Prod.* **16** 198
[37] Moreau E 2007 *J. Phys. D Appl. Phys.* **40** 605
[38] Villermaux J 1993 *Génie de la Réaction Chimique* 2nd edn (Paris: TEC & DOC)
[39] Levenspiel O 1999 *Chemical Reaction Engineering* 3rd edn (New York: Wiley)
[40] Levenspiel O 2012 *Tracer Technology: Modeling the Flow of Fluids* (New York: Springer)
[41] Perry R H, Green D W and Maloney J O 1934 *Perry's Chemical Engineers' Handbook* 7th edn (New York: McGraw-Hill)
[42] Yan K *et al* 2001 *Plasma Chem. Plasma Process.* **21** 107
[43] Schiorlin M *et al* 2009 *Environ. Sci. Technol.* **43** 9386
[44] Harling A M *et al* 2008 *Environ. Sci. Technol.* **42** 4546
[45] Trambouze P 1993 *Réacteurs chimiques—Technologie* https://techniques-ingenieur.fr/base-documentaire/procedes-chimie-bio-agro-th2/reacteurs-chimiques-42330210/reacteurs-chimiques-j4020/ **J4020 v2** 1–31
[46] Takaki K *et al* 2015 *IEEE Trans. Plasma Sci.* **43** 3476
[47] Prantsidou M and Whitehead J C 2015 *Plasma Chem. Plasma Process.* **35** 159
[48] Jiang N *et al* 2015 *J. Phys. D Appl. Phys.* **48** 405205
[49] Gandhi M S *et al* 2013 *J. Taiwan Inst. Chem. Eng.* **44** 786
[50] Delgado J M P Q 2006 *Heat Mass Transf.* **42** 279